



The application of Unmanned Aerial Vehicles (UAVs) to estimate above-ground biomass of mangrove ecosystems



Alejandro Navarro^{a,*}, Mary Young^a, Blake Allan^a, Paul Carnell^b, Peter Macreadie^b, Daniel Ierodiaconou^a

^a School of Life & Environmental Sciences, Faculty of Science, Engineering and Built Environment, Deakin University, Warrnambool 3280, VIC, Australia

^b School of Life & Environmental Sciences, Faculty of Science, Engineering and Built Environment, Deakin University, Burwood 3125, VIC, Australia

ARTICLE INFO

Edited by: Marie Weiss

Keywords:

Mangrove
Unmanned aerial vehicle
Individual tree segmentation
Above-ground biomass
Cost-benefit analysis

ABSTRACT

Mangrove ecosystems are targeted for many conservation and rehabilitation efforts due to their ability to store large amounts of carbon in their living biomass and soil. Traditional methods to monitor above-ground biomass (AGB) rely on on-ground measurements, which are expensive, labour intensive and cover small spatial scales. Structure from Motion and Multi-View Stereo reconstructions from Unmanned Aerial Vehicles imagery (UAV-SfM) have the potential to increase fieldwork efficiency by providing a greater amount of spatial information in less time. However, there is still a need to assess the ability of UAV-SfM to retrieve structural information of mangrove forests, which could pose challenges in areas of high forest complexity and density.

In this study we successfully used UAV-SfM data to estimate height, canopy diameter and AGB of natural and rehabilitated mangrove forests across two regions of the southeastern coast of Australia. We used a variable window filter algorithm to detect trees with an 80% detection rate when considering the top canopy. Individual tree canopy segmentation was performed using a marker-controlled watershed segmentation with two sets of constraining markers: treetops and a minimum height below which a pixel is not considered part of a tree.

Direct comparison with on-ground measurements at the regional level showed no significant difference in tree height and AGB medians when only top canopy was considered. Similarly, median canopy diameters were not significantly different in natural areas of both regions, but significant differences were found in rehabilitated areas. UAV-SfM estimates of AGB were on average 15% lower in natural areas and 10% higher in rehabilitated areas when compared to on-ground measurements and followed a strong linear relationship close to the ideal one-to-one relationship.

Additionally, we performed a cost-benefit analysis of the two methodologies. UAV-SfM methods can save almost AU\$ 50,000 per ha when compared to on-ground measurements and become cost-effective (based on total costs) after just 15 days of surveys. The methods described in this study open the possibility for easily repeatable, low-cost UAV-SfM surveys for local managers by providing a faster, more cost-effective approach for monitoring mangrove forests over larger areas than traditional on-ground surveys while maintaining forest inventory data accuracy in both natural and rehabilitated mangrove forests.

1. Introduction

Mangrove ecosystems provide unparalleled economically and ecologically critical services to coastal areas (Alongi, 2008), including: 1) provisioning (Hemminga and Duarte, 2000); 2) coastal protection (Badola and Hussain, 2005; Das and Vincent, 2009; Koch et al., 2009); 3) recreational and aesthetic uses (Bergstrom et al., 1990); and 4) soil formation and carbon sequestration (Atwood et al., 2017; Donato et al., 2011; Mcleod et al., 2011). Despite their importance they are one of the most threatened and vulnerable ecosystems worldwide (Hamilton and

Casey, 2016; Thomas et al., 2017).

As they occur across the land-sea interface, mangrove forests are subject to both terrestrial and marine pressures. A large percentage of mangrove ecosystems have been altered, destroyed or degraded worldwide as a result of anthropogenic impacts, particularly near populated areas (Clark and Johnston, 2016; Richards and Friess, 2016). Consequently, mangrove ecosystems are the focus for many conservation and rehabilitation efforts (Duncan et al., 2016; Nam et al., 2016; Ren et al., 2010), which require regular monitoring of the forest structure characteristics for better management strategies. This is

* Corresponding author.

E-mail address: ahnnavarr@deakin.edu.au (A. Navarro).

particularly relevant for any projects seeking to gain carbon credits for mangrove rehabilitation under the impacts of climate change related issues (sea level rise and changes in precipitation and temperature; Ward et al., 2016).

Mangrove forest monitoring and management has traditionally relied on regular on-ground surveys for collecting forest inventory data (Nam et al., 2016; Ren et al., 2010). This data collection is important because it provides a better understanding of species composition and carbon biomass of the survey areas. However, these surveys usually cover relatively small spatial scales (< 0.5 ha), and can often be expensive, labour intensive and time-consuming due to the tides, mud, and general difficulty in accessing these remote coastal ecosystems (Lee and Lunetta, 1995).

Remote Sensing data, on the other hand, provides a fast, cost-effective, and efficient method to estimate the biological, biophysical and biochemical factors that translate into some of the services provided by mangrove ecosystems (Giri, 2016; Pham et al., 2019). The type of remote sensing platform (ground-based, airborne or satellite) and sensor (photographic, LiDAR or radar) used depend on the scale and the goal of the research (Wang et al., 2019). Remotely sensed satellite archive data offer broad-scale (nation-wide) and long-term (up to 40 years) monitoring for detection of change over time (Giri, 2016; Kuenzer et al., 2011; Pham et al., 2019). However, it might not necessarily provide the resolution and precision required for local accounting (Ruwaimana et al., 2018). To increase spatial resolution while still covering large areas, airborne LiDAR systems and ground-based platforms like terrestrial laser scanners have been used in the past for retrieval of forest inventory data of coastal wetlands (Feliciano et al., 2014; Wannasiri et al., 2013). However, they are expensive, not widely available, and data management and processing is often difficult and requires specialized software (Wallace et al., 2016; Yin and Wang, 2019).

Unmanned aerial vehicles (UAVs) paired with Structure from Motion and Multi-View Stereo photogrammetric procedures (from now on UAV-SfM) have the potential to: 1) increase fieldwork efficiency by collecting broader spatial information in less time than traditional ground-based surveys (Dandois and Ellis, 2013; Messinger et al., 2016; Murfitt et al., 2017), 2) increase spatial resolution obtained from satellite data while still covering large areas (Ruwaimana et al., 2018), and 3) provide a more cost-effective approach than other airborne systems like LiDAR or airborne photogrammetry while maintaining accuracy and resolution (Dustin, 2015; Sankey et al., 2017).

In terrestrial forests, the implementation of high-resolution imagery collected from low-cost UAVs is becoming an increasingly valuable tool for mapping above-ground carbon stock (Dandois and Ellis, 2010; Samiappan et al., 2016; Zahawi et al., 2015). Common forest inventory data derived from UAV-SfM includes tree species, height, canopy diameter and above-ground biomass (AGB), which can complement, and eventually replace, traditional forest inventory techniques (Dandois and Ellis, 2013; Messinger et al., 2016; Panagiotidis et al., 2017; Zarco-Tejada et al., 2014). Overall, there is a general consensus that UAVs are the most cost-effective solution for sites with an extent between 10 and 20 ha when compared to aircraft and satellite data (Dustin, 2015; Manfreda et al., 2018; Matese et al., 2015). However, no cost-benefit analysis has compared the benefits of using UAVs against on-ground measurements in mangrove ecosystems to date.

Despite the importance of coastal wetlands for carbon accumulation and other ecosystem services, there are few studies evaluating the use of UAV-SfM approaches for assessing the biophysical and biochemical properties of mangrove forests (Li et al., 2016; Navarro et al., 2019; Otero et al., 2018; Tian et al., 2017; Yaney-Keller et al., 2019). Out of these, only two have focused on retrieving mangrove forest inventory data for estimating mangrove AGB (Navarro et al., 2019; Otero et al., 2018). These studies demonstrated that UAV-SfM derived data has the potential for estimating AGB from mangrove plantations, but were unable to predict AGB from natural forests with densely packed mangrove trees. Otero et al. (2018) retrieved information on height from

UAV-SfM data at a plantation and natural site with mixed results (only the height medians from the plantation site were significantly similar). Additionally, validation was achieved through visual interpretation of the orthomosaic, with no direct plot by plot comparison between UAV-SfM and field data. On the other hand, Navarro et al. (2019) managed to perform a tree by tree comparison of UAV-SfM data vs field data for two measurements: height and canopy diameter. However, this study is based on trees from a mangrove plantation project < 8 years old with clearly defined boundaries between trees. Furthermore, only canopy diameter was not significantly different from on-ground measurements. Consequently, the challenge to effectively estimate mangrove AGB from UAV-SfM derived forest inventory data still remains.

In this study, we propose an approach that combines tree detection and canopy segmentation algorithms applied to UAV-SfM data for quantifying AGB of mangrove forests within natural and rehabilitated (25+ years) areas of the southeastern coast of Australia, and compare it to on-ground measurements at the plot level. Moreover, we perform the first cost-benefit analysis to date of the two different methods (field based measurements vs UAV-SfM data) in mangrove ecosystems to estimate above-ground biomass. The methods described in this study provide local managers with a cost-effective approach for regular monitoring of mangrove forests over larger areas than traditional on-ground surveys while maintaining forest inventory data accuracy.

2. Materials and methods

2.1. Study area

We focused our research on two areas of the southeastern coast of Australia: Western Port (WP) in southern Victoria (Fig. 1b) and Richmond River Estuary (RRE) in northern New South Wales (Fig. 1c). WP is a large tidal bay that covers around 680 km², of which 270 km² are exposed mudflats at low tide. Mangrove ecosystems in WP are located near the southernmost distribution of mangrove ecosystems in the world and cover an area of around 1800 ha (Boon et al., 2011, Fig. 1d). Air temperatures in WP can be as low as 0 °C during winter, making mangrove survival very difficult (Macnae, 1966). As in most temperate climates, the mangrove forests in this region are structurally homogeneous (only one species: *Avicennia marina*) and are considered shrub or dwarf mangroves as their height only ranges from 1 to 3.5 m (Vandervalk and Attiwill, 1984).

Mangrove forests in RRE, although still dominated by *A. marina*, are more structurally complex, both in diversity (up to 3 other species: *Aegiceras corniculatum*, *Bruguiera gymnorrhiza* and *Excoecaria agallocha*) and height range (from 2 m up to 17 m). RRE is one of the major coastal drainage systems in northern NSW with a catchment area of approximately 6850 km² of which approximately 600 ha is mangroves (Russell, 2005). A substantial part of this area consists of restoration projects dating as far back as 1991. Mangrove forests on these rehabilitated areas usually have two distinct canopy stories: an upper one between 4 m and 8 m of height formed mainly by *A. marina*, and a lower one at around 2 m dominated by *A. corniculatum*. UAV-SfM and on-ground surveys were conducted at both natural and rehabilitated areas (Fig. 1e).

2.2. Methods

We used a low cost UAV and the in-built RGB sensor to detect and measure the structural characteristics of individual trees within mangrove ecosystems in southeastern Australia. Along with the UAV imagery, we collected ground data and validated the algorithm for estimating number of trees, height, canopy diameter and above-ground biomass. The workflow outlined in Fig. 2 was created to evaluate the potential use of UAV-SfM to retrieve structure characteristics of the mangrove forest.

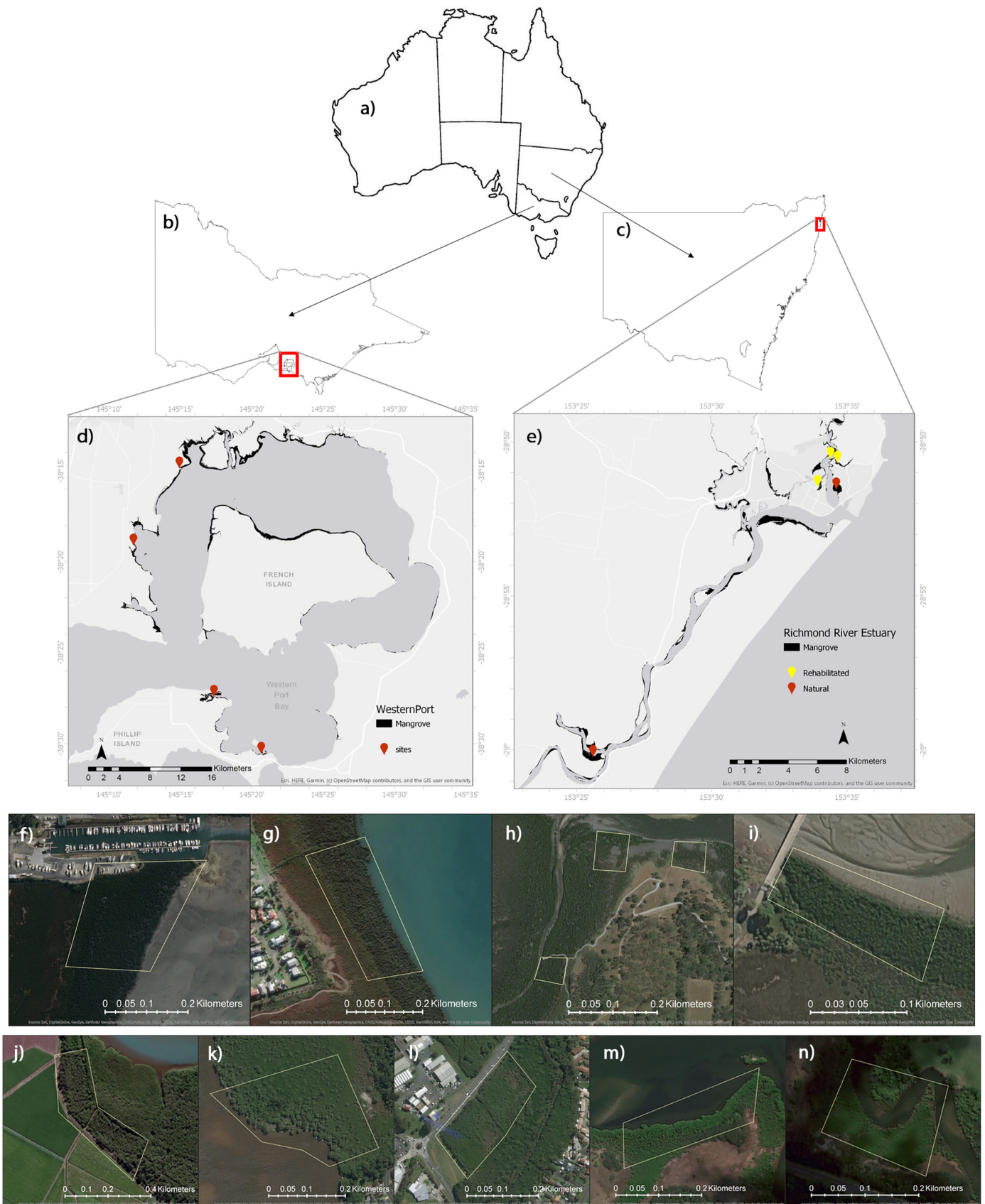


Fig. 1. Location of the two study areas: d) Western Port, Victoria (b) and e) Richmond River Estuary, New South Wales (c). The red and yellow pins mark the areas where UAV-SfM and field data were collected (Natural and Rehabilitated areas respectively). Water in dark grey, land in light grey and mangrove extent distribution in black. f-n) zoomed in images over areas of interest (f-i Western Port; j-k Richmond River Estuary Natural areas and l-n Richmond River Estuary Rehabilitated areas). White polygons show area surveyed by the UAV. Maps created using ArcGIS Pro (v.2.1.1; esri.com). (For interpretation of the references to color in this figure legend, the reader is referred to the web version of this article.)

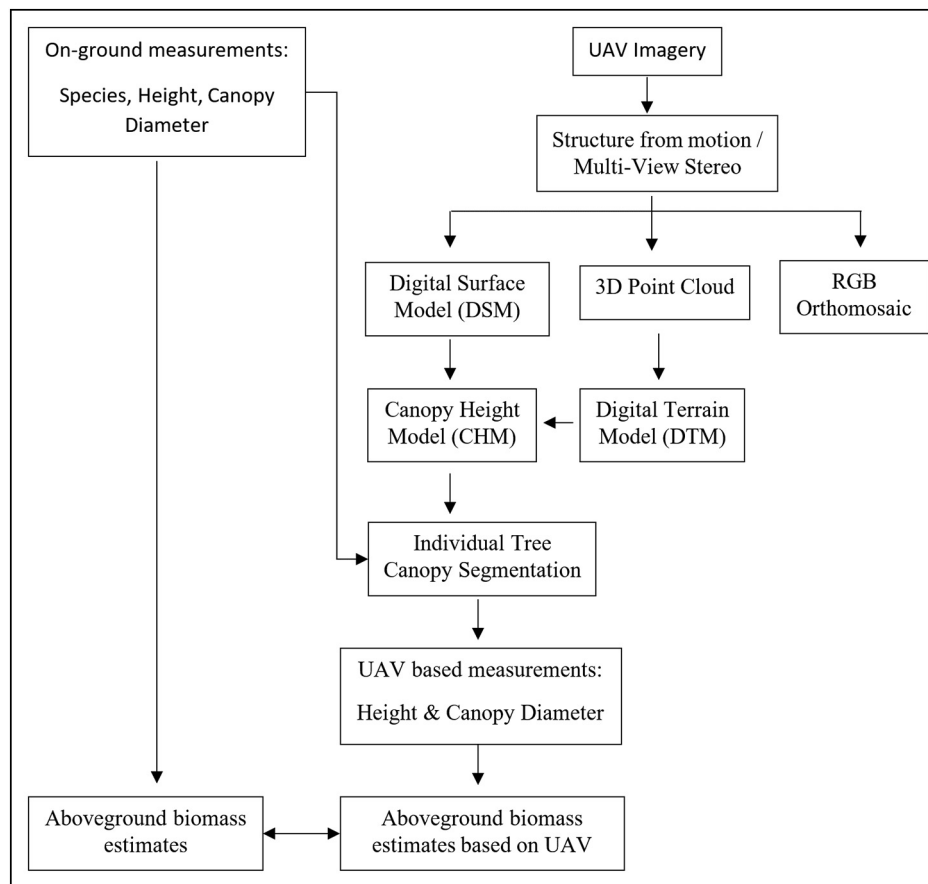


Fig. 2. Workflow to evaluate the potential use of UAV-SfM based methods to estimate above-ground biomass of mangrove ecosystems in southern Australia.

2.2.1. Forestry field methods

Including both regions, a total of 9 survey areas and 41 plots (Fig. 1) were located along a transect parallel to the coastline (at approximately 30 m intervals). In Richmond River Estuary, a total of twenty 10×10 m plots were distributed into five survey sites (three in rehabilitated areas and two in natural areas). The remaining 21 plots were distributed into four survey sites in Western Port. Plot size in WP was reduced to 10×2 m due to the higher mangrove vegetation density typical of shrub/dwarf mangrove forests. Results are still comparable as AGB was standardised to t/ha for analysis. We geolocated the four corners of each plot using a real time kinematic global positioning system (RTK GPS; Emlid Reach RS using the GPSnet-VIC and CORSnet-NSW base station networks) with 3 cm horizontal accuracy and 6 cm vertical accuracy.

Forest inventory data were collected between March and May 2017. In each plot, we measured the height, basal diameter, stem diameter and average canopy diameter (calculated as the mean of the greatest canopy width and its perpendicular canopy width) of every adult tree. Heights under 2 m were measured using a tape measure, while heights over 2 m were recorded using a compact laser rangefinder. When the number of trees of a single species exceeded 50 trees per plot and trees were homogeneous in height and canopy diameter (as it is often the case of *A. corniculatum* on rehabilitated areas of RRE), all trees were counted and a randomly selected subsample of 25 trees was measured.

2.2.2. UAV image acquisition

We acquired imagery data between January and May 2018 using a DJI Phantom 4 Advanced quadcopter and the in-built 20 MP RGB camera. The flight missions were designed using Pix4DCapture software (Pix4D SA, Lausanne, Switzerland) in a cross-grid pattern to ensure a better reconstruction of the 3D models (Nesbit and Hugenholtz, 2019).

We flew each site at an altitude of 30 m above the ground with 85% overlap and 70% sidelap and covered an area of approximately 1 ha around each plot. Surveys were restricted to days with low wind speed (< 15 knots or 7.7 m/s), no rain, and low tides to ensure weather conditions did not interfere with data collection and processing.

Prior to flying, between 10 and 15 black and white checkerboard targets were evenly placed at each site on the ground in open areas, and marked with the RTK GPS to be used as ground control points (GCPs) for accurate geo-referencing of the imagery.

2.2.3. Field data processing

Field-derived mangrove above-ground biomass was estimated at the tree level using species-specific allometric equations for every dominant structural form (tall vs shrub/dwarf mangroves) and species. As height and canopy diameter are the only variables that can be obtained using the UAV-SfM method, all the allometric equation chosen for this study were derived using a combination of these two variables, which did not interfere with our ability to estimate mangrove AGB (R^2 0.96–0.99). In WP, we used the allometric equation provided by Owers et al. (2018; Table S2b: Region-specific equation for *A. marina* using only Height and Crown area: $AGB = \exp(-5.39183 + 1.1847751 * \log(H) + 1.1417521 * \log(CA)) * 1.088$; where H is Height in cm and CA is Crown Area in m^2) for all adult mangroves. Whereas in RRE, the methods used by Fu and Wu (2011) were applied for both *A. marina*, *B. gymnorhiza* and *E. agallocha* (similar morphology; $AGB = 1.8247 * (CD^2 * H)^{1.0202}$) and *A. corniculatum* ($AGB = 3.1253 * (CD^2 * H)^{0.9063}$; where CD is average Canopy Diameter in m and H is Height in m).

2.2.4. UAV data processing

Structure from Motion and Multi-View Stereo (SfM-MVS) procedures were implemented within Pix4Dmapper software (v. 4.2.26,

Pix4D SA, Lausanne, Switzerland) to create a 3D point cloud (average density: > 4000 points/m³), a Digital Surface Model (DSM, Model depicting elevations of the top of reflective surfaces, such as vegetation) and an orthomosaic image (both with an average ground sampling distance of 0.8 cm per pixel). The SfM-MVS reconstruction works by identifying and automatically tying keypoints on a set of overlapping images (median of $\sim 70,000$ keypoints per image). A self-calibrating bundle adjustment is then used to calibrate the camera parameters of each image and derive a sparse set of 3D keypoints, which is then refined using MVS techniques to generate high resolution densified point cloud and estimate the 3-D point positions (Dandois and Ellis, 2010; Westoby et al., 2012).

We manually identified and marked the GCPs in all available images for high precision geo-referencing of all products. This allowed for the corners of the on-ground survey plots to be located with high precision for posterior comparison of tree metrics and above-ground biomass estimates.

A Digital Terrain Model (DTM, a model depicting the geodesic surface or bare land devoid of vegetation) was created by spatial interpolation of the visible ground points (3D points intersecting the bare land) at every survey site using a k-nearest neighbour approach with an inverse-distance weighting (Number of k-nearest neighbours: 1000; Power for inverse-distance weighting: 2). A randomly selected subset of 15% of the points from the 3D point cloud (~ 700 points/m³) was used for classification into ground/not ground points using the progressive morphological filter developed by Zhang et al. (2003) with a variable window size (0.6, 1.4, 3.8, 11.0 and 32.6 m). The low gradient slope natural to these ecosystems allowed us to choose very restrictive threshold heights for every window size (0.05, 0.07, 0.11, 0.23 and 0.59 m, respectively) to effectively eliminate as much of the elevation values intersecting vegetation as possible. The accuracy of the DTM was evaluated using the Root Mean Square Error (RMSE) between the height of the DTM and the correspondent height value from the GCPs.

Finally, we developed Canopy Height Models (CHM, a model of the relative height of the trees within the study area) at an average resolution of 3.2 cm by subtracting the DTM values from the DSM using max height metric. All 3D point cloud computations were performed using the R package 'lidR v2.0.0' (Roussel and Auty, 2018). From the CHMs, the following steps were performed for individual tree canopy segmentation of every mangrove tree within the plots:

Step 1: The tree tops were detected using a local maximum function that implements the variable window filter algorithm developed by Popescu and Wynne (2004). A cell is tagged as a tree top when it is the highest within the window. To compensate for varying canopy sizes, the size of the moving circular window changes depending on the height of the cell on which it is centered. The function used to determine the variable window size was defined using the best fitting model of the height and associated mean canopy diameter values obtained from the on-ground data (Fig. 3). A different function was used for WP (Fig. 3a), rehabilitated areas of RRE (Fig. 3b) and natural areas of RRE (Fig. 3c).

Step 2: Individual tree canopy segmentation was performed to outline crown shapes from the CHM using a marker-controlled watershed segmentation (Vincent and Soille, 1991) from the 'imager' R package (Barthelme, 2018). The watershed transform is a label propagation algorithm controlled by a priority map (using the treetop locations as seeds from which the objects can propagate). Neighbouring pixels around the treetop will be added to the object/tree until another object/tree or background is met.

Step 3: To avoid tagging underlying bush or saplings as part of the main canopy of the mangrove trees, pixels below 0.8 times the maximum height of each tree were removed (Panagiotidis et al., 2017). We determined this threshold value by testing a range of different height values (0.5 to 0.9 times at 0.1 intervals). However, in sites where two differentiated canopy stories co-exist (typically those in the rehabilitated areas of RRE, with height differences of > 1 m), a different

value was chosen for the upper and lower canopy (0.6 and 0.8 times, respectively).

Step 4: Preliminary visual analysis identified the potential for canopies of smaller overlapping trees to be omitted after Step 3. Therefore, already detected tree canopies were buffered by 10 cm and masked out from the CHMs and steps 1 to 3 were then repeated over the remaining area to identify the potentially omitted tree canopies. A buffer was necessary so that no immediate points around a tree (which will be higher than neighbouring pixels if maximum crown was not found within the top 20% of the tree height) were picked as treetops. We tested 5, 10 and 20 cm buffers and found 10 cm to be the best buffer (thin enough to not cover omitted trees and wide enough so that no immediate points were picked as treetops). Extra iterations were not necessary.

Step 5: Next, mangrove trees were discarded if: a) 50% or more of their canopy fell outside the plot area; or b) their maximum height was below 1 m (for WP, except for one plot where all tree heights ranged between 0.7 and 1 m) and 1.3 m (for RRE). This height threshold was chosen as a cut-off to separate adult mangrove trees from saplings and was based on field data.

Step 6: Two measurements were then retrieved for canopy diameter: the maximum width spanning the convex hull of a tree crown (calculated as the maximum distance between vertices) and the maximum width distance that is perpendicular to the previous measurement (adapted from 'lakeMaxWidth' function from 'lakemorpho' R package, Hollister, 2018).

Step 7: Finally, mangrove AGB was estimated at the tree level using the same species-specific allometric equation as with the on-ground measurements. In WP, we used the allometric equation provided by Owers et al. (2018, Table S2b: Region-specific equation for *A. marina* using only Height and Crown area). In RRE, the same allometric equation was used for *A. marina*, *B. gymnorrhiza* and *E. agallocha* (similar morphology, Fu and Wu, 2011). *A. corniculatum* was only present on rehabilitated areas of RRE and formed a differentiated canopy story from the other 3 species (two to four meters lower in height). In these areas, mangrove trees were separated into two categories according to their height (based on field data) and a different allometric equation was applied to *A. corniculatum* (Fu and Wu, 2011).

2.2.5. Statistical analyses

Mangrove tree density and height, canopy diameter and AGB medians estimated from the UAV-SfM were compared to field data at the plot level using linear regression models. A Shapiro-Wilk test (Shapiro and Wilk, 1965) was used to test for normality of mangrove tree height, canopy diameter and AGB distributions at the region level. As all distributions were significantly different than normal distribution (p -value < 0.05), a non-parametric test (Wilcoxon Rank-Sum test; Wilcoxon, 1992) was used to compare UAV-SfM derived height, canopy diameter and AGB medians to those measured in the field at the plot level (an alpha level of < 0.05 was chosen as a cut-off to reject the null hypothesis: the two samples come from the same distribution). All analyses were performed using both: all trees measured and trees only visible from the UAV point of view. All data processing and statistical analyses were performed using R software (version 3.5.1; <http://www.r-project.org/>).

2.2.6. Cost-benefit analysis

Two components were used for the cost-benefit analysis: costs associated with each method, and benefit assessment which was based on cost savings, strengths and limitations of each method for AGB estimation.

The cost for both methods incorporated three main components: equipment (including software requirements); data acquisition and preparation; and data processing and analysis. A summary of how the costs were estimated for each component/subcomponent of both methodologies can be found in Table 1. Costs were estimated in AU\$/ha

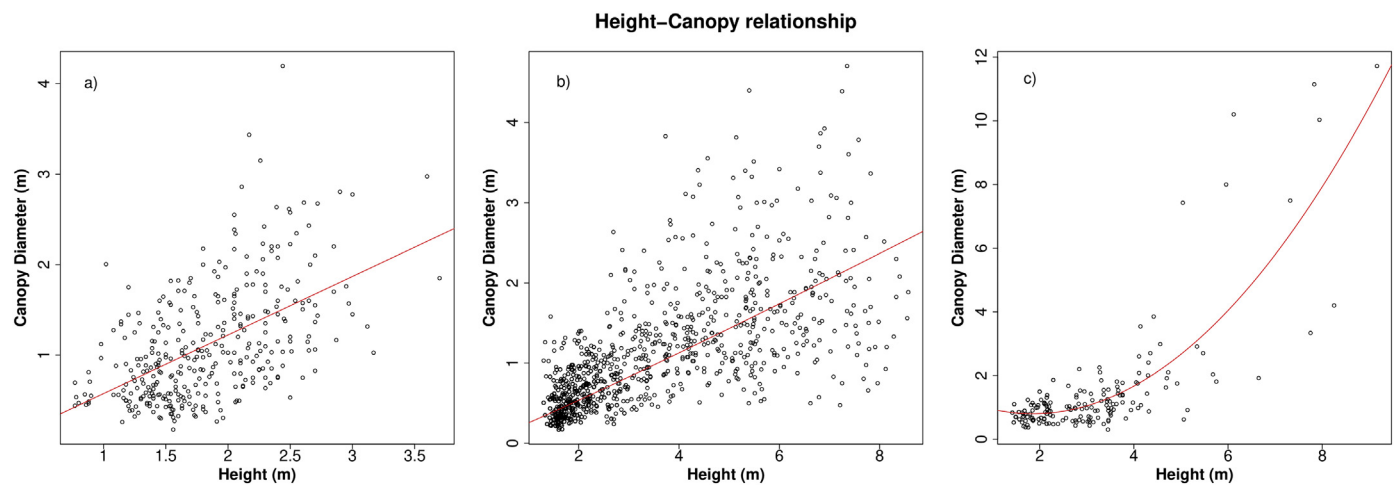


Fig. 3. Relationship between Canopy Diameter (measured as the mean of the greatest canopy width and its perpendicular canopy width) and Height from the on-ground measurements for a) WP: $ws = 0.647 * H - 0.073$; b) RRE rehabilitated areas: $ws = \exp(1.071 * \ln(H) - 1.365)$; and c) RRE natural areas: $ws = 0.189 * H^2 - 0.702 * H + 1.453$; where $ws =$ Window Size (m) and $H =$ Height (m).

and based on the average annual salary of a Research Assistant in Australia (AU\$ 34.11 per hour) and on 100 days of surveys (based on estimated UAV lifespan of 200 flight hours (*pers. obs.*) at an average of 2 flight hours per day). These monetary costs are compared to determine the financial benefit of the UAV-SfM method.

Human resources for fieldwork were estimated based on a team of 2 people (for UAV surveys) and 5 people (for on-ground measurements) and 8 h of work per day. A UAV-SfM data acquisition operation consisted of flight planning, GCP deployment and RTK marking and UAV flight. Total time for a single UAV operation was less than an hour and covered an area of approximately 1 ha of forest. On-ground data acquisition consisted of plot delineation and forest inventory data collection and took an average of 2.5 h per plot (100 m², estimates based on the time it took a team of 5 people to survey the 41 plots present in this study).

Human resources for data processing and analysis were estimated based on 1 person for both methodologies. UAV-SfM data processing and analysis consisted of: 1) GCP rectification; 2) Point cloud cleaning; and 3) Model application. Each component takes approximately 15 min per ha surveyed. The costs of doing the first survey of on-ground measurements (a total of 0.2 ha) for the UAV-SfM model calibration (function used for variable window filter in Step 1 and species composition) were also included into the UAV-SfM costs. On-ground data processing consisted of data entry and took an average of 1 h per 100 m² surveyed.

Table 1
Components and subcomponents used for estimating the costs for each AGB estimation method.

Component	Subcomponent	Detailed costs	
		UAV-SfM method	Field data method
(1) Equipment	Equipment	UAVs (2 DJI Phantom 4 Pro + 4 Batteries + 2 iPad Mini + 1 DJI Battery Charger + 4 sets Propellers + 4 micro SD cards) RTK GPS (1 Emlid Reach RS)	Tape measures Rangefinder
	Software	Pix4D License	NA
(2) Data acquisition and preparation	Data acquisition	Flight planning	Plot delineation
		GCP marking	On-ground measurements
		UAV flight	Vehicle lease cost
		Vehicle lease cost	Fuel cost
		Fuel cost	
(3) Data processing and analysis	Data processing	GCP rectification	Data entry
		Point cloud cleaning	
	Data analysis	Model application Allometric equations	Allometric equations

3. Results

3.1. UAV-SfM derived point clouds and Canopy Height Models

An average of 250 images per hectare were used to generate the dense point clouds using SfM-MVS procedures. An orthomosaic image, DSM, DTM and CHM were generated for every survey site with an average pixel resolution of 3.2 cm (Fig. 4). The geometric accuracies of the scene reconstructions averaged an RMS horizontal error (x, y) of 1.0 cm and RMS vertical error (z) of 1.2 cm. DTM generation averaged a RMSE vertical error of 6.3 cm for WP, 9.0 cm for RRE (rehabilitated areas) and 44.7 cm for RRE (natural areas) when compared to GCPs.

Mangrove trees in WP showed a homogeneous profile of heights due to the slow growth rate characteristic of temperate climates, with trees ranging from 1 to 3.5 m (Vandervalk and Attiwill, 1984, Fig. 4d). This disposition allowed for almost all trees to be visible from UAV imagery, with only saplings and 5% of adult trees under the main canopy not recorded. On the other hand, mangrove trees in RRE showed a more heterogeneous profile of heights, especially in rehabilitated areas where two differentiated canopy stories can be found (Fig. 5). This variation in canopy heights results in a relatively large percentage of the mangrove trees from the lower canopy story not observable from the UAV (up to 30% in some rehabilitated areas). Even though this is a large percentage of trees not being detected by the UAV-SfM method, these trees only hold an average of 9.1% of the total plot-level AGB.

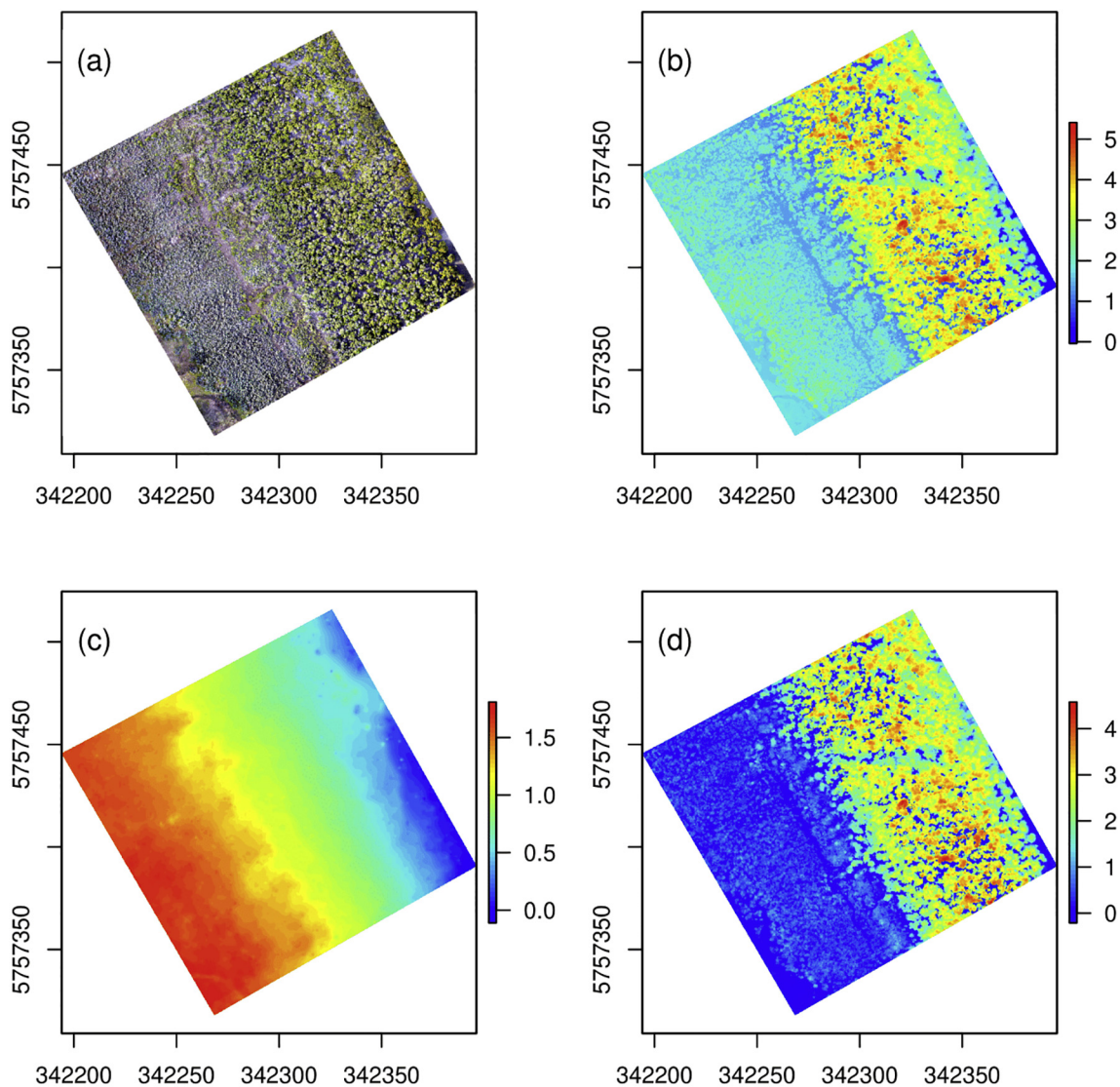


Fig. 4. UAV-SfM data derived products: (a) Orthomosaic image; (b) Digital Surface Model; (c) Digital Terrain Model and (d) Canopy Height Model. Units are expressed in meters.

3.2. CHM derived forest inventory data

3.2.1. Number of trees

Results of the validation work that consisted of comparing on-ground measured tree densities to UAV-SfM derived tree densities for each of the 41 plots can be seen in Fig. 6. When considering only the top canopy (Fig. 6b), the method performed well at low tree densities (< 0.8 trees per m^2), but oversaturated at higher tree densities, following an exponential relationship with an adjusted coefficient of determination of 0.82 and p -value < 0.001 .

3.2.2. Height and canopy diameter metrics

The mangrove tree height, mean canopy diameter and biomass data measured in the field and from the CHMs are summarized in Table 2.

In WP, the tree heights from the on-ground measurements ranged between 0.77 and 3.70 m, with a median height of 1.80 m. For the CHM-based measurements, tree heights ranged between 0.71 and 3.33 m, with a median height of 1.80 m. The two distributions were not significantly different (Wilcoxon Rank-Sum test, p -value = 0.389).

When considering all surveyed trees from the on-ground measurements in RRE, the tree heights ranged between 1.3 and 12.4 m, with a median height of 2.00 m. This value was found to be significantly

different than the one obtained from the CHM-based measurements (2.12 m; Wilcoxon Rank-Sum test, p -value = 0.013). However, when considering only the top canopy, median tree height for on-ground measurements was 2.30 m, which was not significantly different from the CHM-based measurements (2.64 m; Wilcoxon Rank-Sum test, p -value = 0.889).

In WP, the mean Canopy Diameters measured from the on-ground data ranged between 0.18 and 4.2 m, with a median measurement of 0.98 m. For the CHM-based measurements, Canopy Diameters ranged between 0.27 and 3.75 m, with a median measurement of 1.02 m. The two distributions were not significantly different (Wilcoxon Rank-Sum test, p -value = 0.254).

When considering all surveyed trees from the on-ground measurements in RRE, the tree canopy diameters ranged between 0.17 and 11.7 m, with a median canopy diameter of 0.62 m. This value was significantly different than the one obtained from the CHM-based measurements (0.80 m; Wilcoxon Rank-Sum test, p -value < 0.001). Similarly, when considering only the top canopy, median tree height for on-ground measurements was 0.71 m, which was also significantly different from the CHM-based measurements (0.89 m; Wilcoxon Rank-Sum test, p -value < 0.001). Further analysis revealed that, while the medians based on the CHMs and field data for the rehabilitated areas

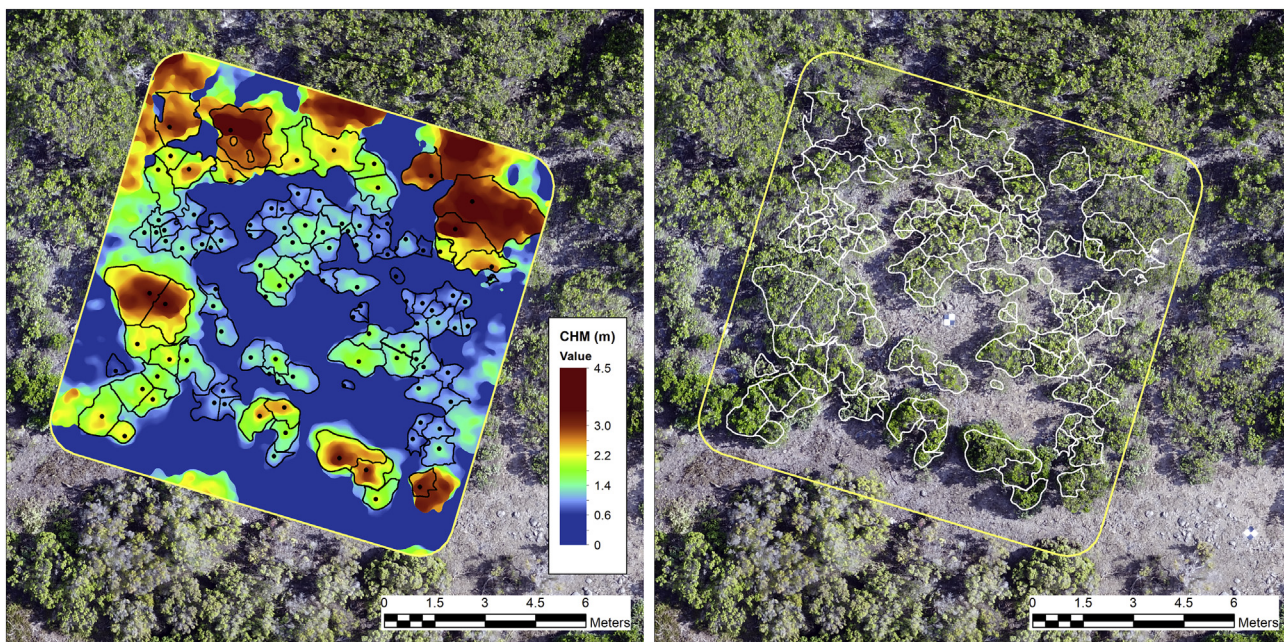


Fig. 5. Final products showing a heterogeneous profile of heights with two distinct canopy stories: (a) Canopy Height Model (CHM) showing individual treetop locations (black dots) and associated tree crown perimeter (black line) measured using the UAV-SfM method. (b) High definition orthomosaic image with crown perimeters in white.

where still significantly different (Wilcoxon Rank-Sum test, p -value < 0.001), the medians for the natural areas were not significantly different when considering only the top canopy (Wilcoxon Rank-Sum test, p -value = 0.602).

Results of the validation work that consisted of comparing on-ground height and canopy diameter medians to UAV-SfM derived estimates (in cm) for each of the 41 plots can be seen in Fig. 7. Strong correlations close to the one-to-one linear relationship (adjusted coefficient of determination of 0.946 and 0.835 respectively) can be found when trees under the main canopy are removed from the analysis (Fig. 7b and d).

3.2.3. Above-ground biomass

Estimated AGB based on the UAV-SfM data in WP and natural areas of RRE was consistently lower (between 10 and 20%) than that generated from the field data at each survey site (Table 2). We observed the opposite pattern in the rehabilitated areas of RRE, where AGB estimates from UAV-SfM data were consistently higher (~10%) than those from field measurements when only the top canopy was considered (Table 2). In WP, the estimated tree AGB median from the on-ground measurements was 0.74 Kg. This value was not significantly different than the value obtained from the CHM-based measurements (0.66 Kg; Wilcoxon Rank-Sum test, p -value = 0.924).

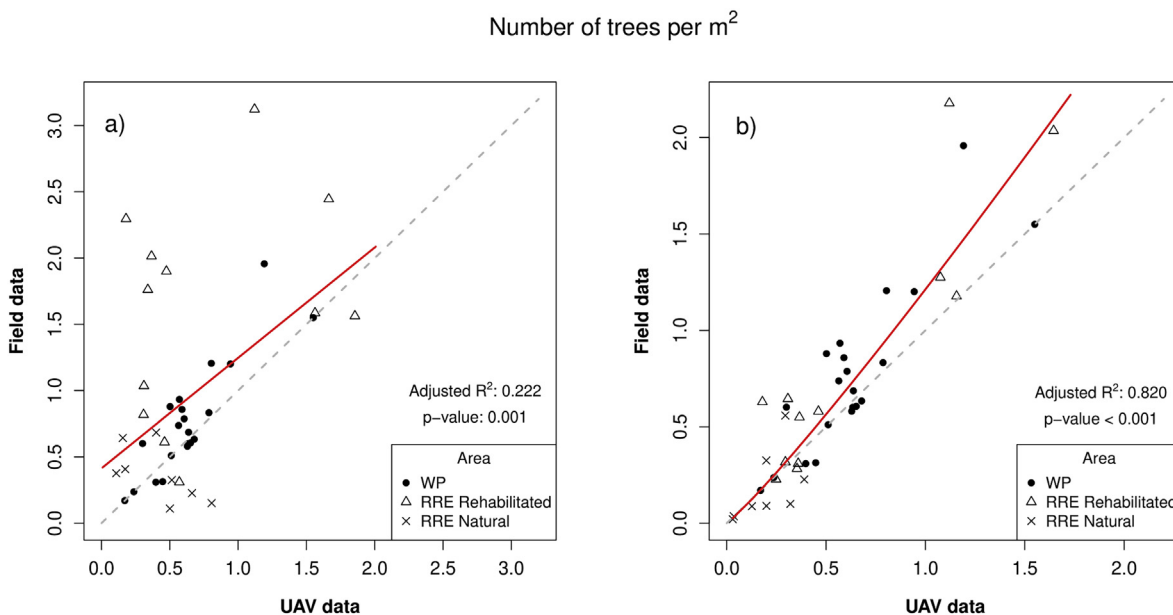


Fig. 6. Comparison between the average number of trees per ha identified by the watershed algorithm and the field data at the plot level using: a) All data and b) Top Canopy data. The dashed line indicates the ideal one-to-one relationship between the two datasets. The red line corresponds to the fitted relationship between the two data sets (for only Top Canopy: $y = \exp. (1.104 * \ln (x) + 0.193)$). (For interpretation of the references to color in this figure legend, the reader is referred to the web version of this article.)

Table 2
Summary of mangrove tree height and mean Canopy Diameter data measured in the field and from the UAV-SfM data.

Area	Method	N	Height (m)			Canopy diameter (m)			AGB (t/ha)
			Min	Median	Max	Min	Median	Max	
WP	On-ground	344	0.77	1.80	3.70	0.18	0.98	4.20	13.6
	UAV-SfM	283	0.71	1.80	3.33	0.27	1.02	3.75	11.2
RRE (All Trees)	On-ground	2220	1.30	2.00	12.4	0.17	0.62	11.7	163.9 / 257.9 ^a
	UAV-SfM	1274	1.30	2.12	13.8	0.25	0.80	9.2	152.1 / 230.6 ^a
RRE (Top Canopy)	On-ground	1155	1.30	2.30	12.4	0.17	0.71	11.7	129.4 / 239.6 ^a
	UAV-SfM	917	1.30	2.64	13.8	0.25	0.89	9.2	149.5 / 214.4 ^a

^a Rehabilitated areas on the left and natural areas on the right.

When considering all surveyed trees from the on-ground measurements in RRE, the tree AGB median was 3.48 Kg, which was significantly different than the value obtained from the CHM-based measurements (3.18 Kg; Wilcoxon Rank-Sum test, p-value = 0.009).

However, when considering only the top canopy, median tree AGB for on-ground measurements was 3.85 Kg, which was not significantly different from the CHM-based measurements (4.19 Kg; Wilcoxon Rank-Sum test, p-value = 0.163).

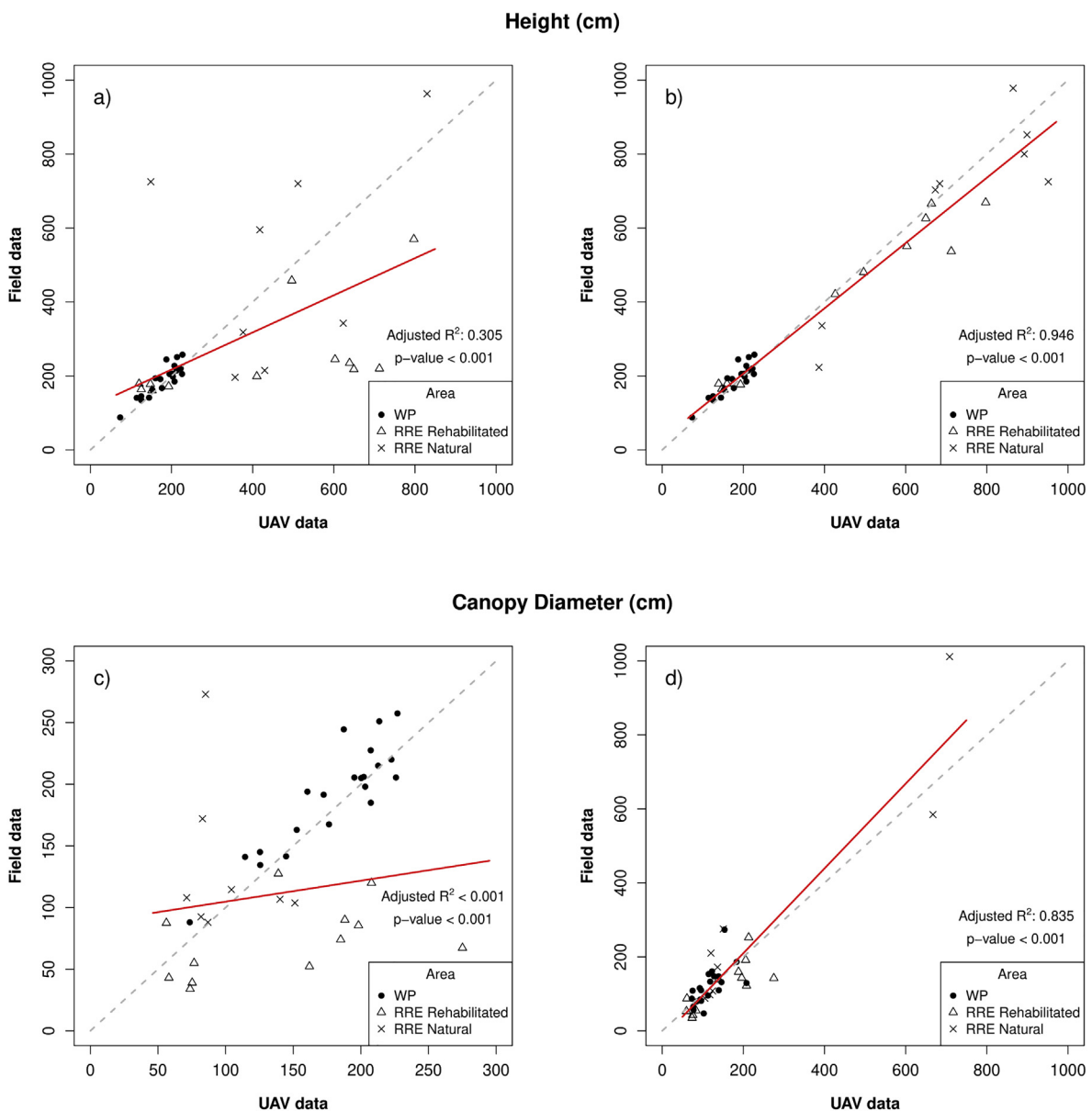


Fig. 7. Comparison between the median heights (a and b) and median canopy diameters (c and d) from UAV-SfM data and the on-ground measurements at the plot level using: All data (a and c) and Top Canopy data (b and d). The dashed line indicates the ideal one-to-one relationship between the two datasets. The red line corresponds to the fitted relationship between the two data sets. (For interpretation of the references to color in this figure legend, the reader is referred to the web version of this article.)

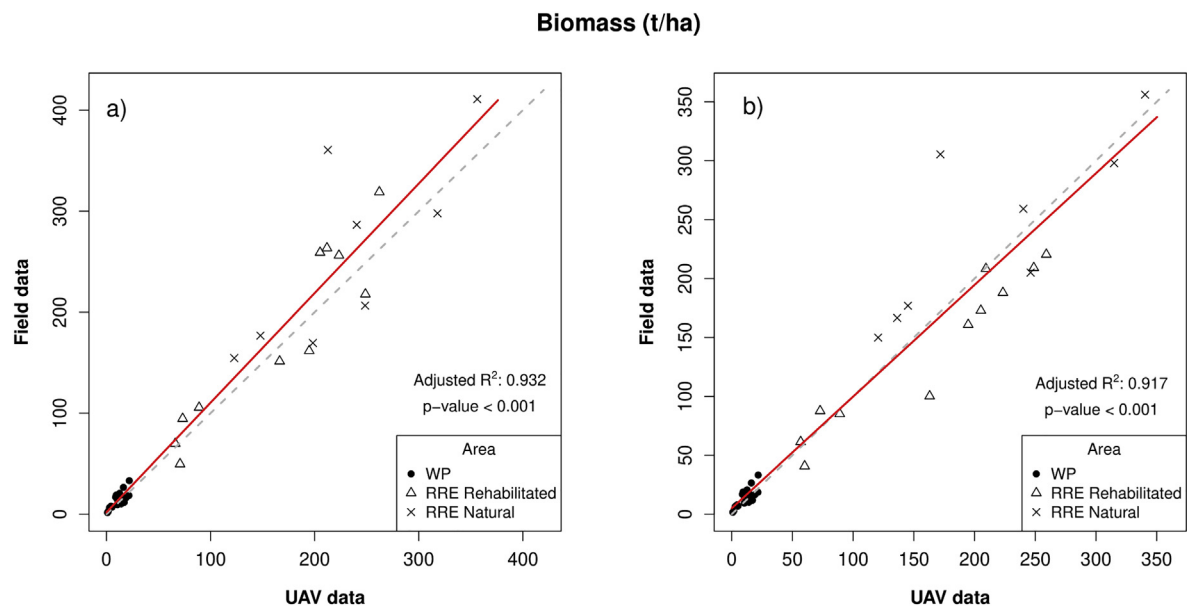


Fig. 8. Comparison between the above-ground biomass estimates (in tonnes per ha) from UAV-SfM data and the on-ground measurements at the plot level using: a) All data and b) Top Canopy data. The dashed line indicates the ideal one-to-one relationship between the two datasets. Whereas the red line corresponds to the fitted linear relationship between the two data sets (for only Top Canopy: $y = 0.948 * x + 4.997$). (For interpretation of the references to color in this figure legend, the reader is referred to the web version of this article.)

Results of the validation work that consisted of comparing on-ground AGB estimates to UAV-SfM derived estimates (in tonnes per hectare) for each of the 41 plots using both all data and only top canopy can be seen in Fig. 8. Both models showed a strong correlation between the two data sets (adjusted coefficient of determination of 0.932 and 0.917 respectively).

3.2.4. Cost-benefit analysis

The equipment, time and costs required for completing the data acquisition, processing and analysis for both methodologies were tallied separately in Table 3. After 100 days of surveys, the UAV-SfM method can cover an area of 800 ha using a total of 1600 person-hours of data acquisition and 600 person-hours of data processing and analysis. In contrast, the on-ground surveys could only cover 3.2 ha of forest using 4000 person-hours of data acquisition and 300 person-hours of data processing and analysis.

The results of the analysis show that the UAV-SfM method has the

Table 3

Detailed costs and total cost in Australian dollars (AU\$) for both forest inventory data collection methods. Costs were based on 100 days of surveys (average lifespan of UAV equipment) and the average annual salary of a Research Assistant in Australia (AU\$ 70,953).

Component	Detailed costs	
	UAV-SfM method	Field data method
Equipment	UAVs: AU\$ 6364 RTK GPS: AU\$ 1150 Pix4D License: AU\$ 2770	Tape measures: \$124 Rangefinder: \$600
Data acquisition and preparation	staff salaries: AU\$ 58,480 vehicle hire cost: AU\$ 6500 fuel cost: AU\$ 3500	staff salaries: AU\$ 136,000 vehicle hire cost: AU\$ 6500 fuel cost: AU\$ 3500
Data processing and analysis	staff salaries: AU\$ 21,012	staff salaries: AU\$ 10,200
Total	AU\$ 99,884	AU\$ 156,924
Total (per ha)	AU\$ 125	AU\$ 49,039

potential to save a total of AU\$ 57,040 per 100 survey days or AU\$ 48,914 per ha surveyed (Table 3). Field data offers AU\$ 10,160 on savings in terms of equipment (including software) when compared to UAV-SfM methodology. However, staff salaries for data acquisition and processing of on-ground measurements were almost double those of the UAV-SfM methodology for the same category (AU\$ 156,200 vs AU\$ 89,492 respectively). A day by day cost analysis revealed that the UAV-SfM method is more expensive than on-ground surveys during the first 14 days of surveys, but becomes cost-effective on day 15 (AU\$ 23,816 vs AU\$ 24,154 respectively, Fig. 9).

4. Discussion

This study has demonstrated the ability of UAV-SfM data to estimate AGB of mangrove ecosystems. Low-cost UAV imagery was used for the creation of orthomosaic images, DSM, DTM and CHMs for nine survey sites in the southeastern coast of Australia using Structure from Motion procedures. There was a close correspondence between UAV-SfM derived tree heights, average canopy diameters, tree density and ultimately AGB estimates with those measured in the field. Other studies have found that UAV-SfM data can be used as a tool for the retrieval of vegetation structure characteristics (Dandois and Ellis, 2010; Messinger et al., 2016; Panagiotidis et al., 2017; Zarco-Tejada et al., 2014). However, very few have attempted to estimate AGB of mangrove ecosystems from UAV-SfM derived CHMs due to the high tree density and overlap of these ecosystems (Navarro et al., 2019; Otero et al., 2018). Moreover, the use of UAV imagery is less expensive than on-ground measurements (Table 3), manned flights imagery (Dustin, 2015; Matese et al., 2015) and LiDAR systems (Sankey et al., 2017) while maintaining forest biomass estimation accuracy.

4.1. Comparison between UAV-SfM and field data derived metrics

Out of the 344 trees measured in the field for WP, 82% (283 trees) were detected using the UAV-SfM methods described in this study. A similar value (79%) was obtained for RRE when only the top canopy was considered (915 out of 1148). This value is consistent with other studies with similar methods for tree detection from SfM derived products on high tree density forests (64%–96% Nevalainen et al., 2017;

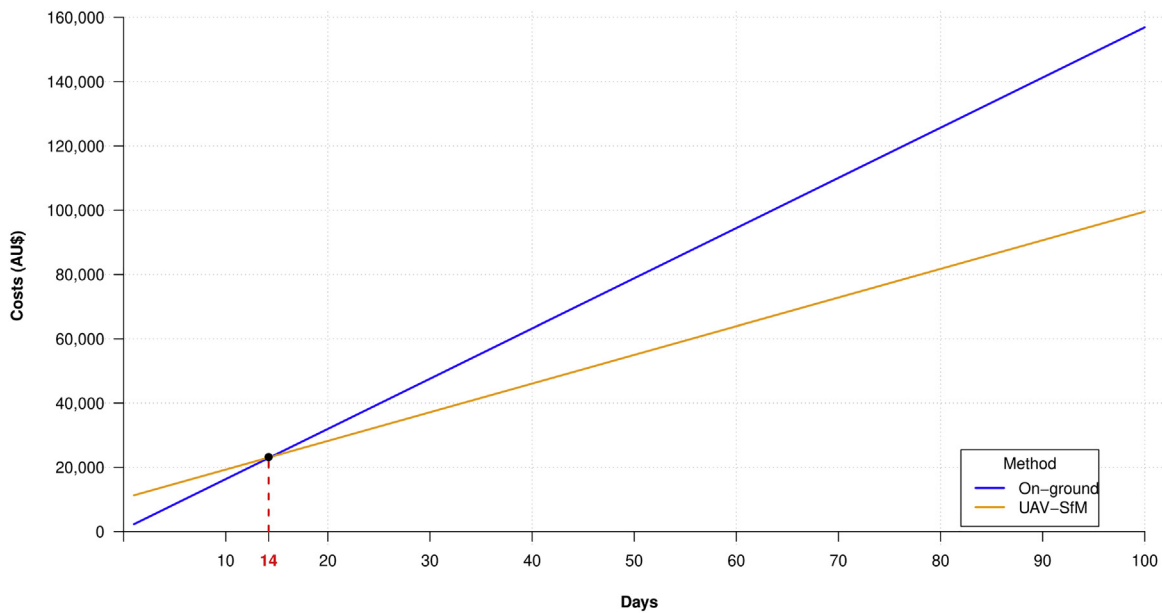


Fig. 9. Comparison of costs per days of survey (in AU\$) between the on-ground and the UAV-SfM methods.

82% in Wallace et al., 2016). This level of underestimation is within accepted levels for forestry and carbon inventory needs (Sperlich et al., 2014). The number of trees detected dropped to 57% when all trees were considered for RRE (Table 2), however, this large number of non-detected small trees, only accounts for an average of 9.1% of the total biomass.

When considering only the top canopy, the method performed well at low tree densities (< 0.8 trees per m^2), but oversaturated at tree densities over 0.8 trees per m^2 and deviated from the one-to-one relationship with on-ground data following an exponential curve (see Fig. 6b). Canopies of trees of similar height to neighbouring trees often intertwine in high tree density areas, resulting in the omission of trees with highly overlapping crowns from UAV-SfM derived estimates. Similarly, the smaller overlapping trees under the main canopy are often not visible from the UAV point of view and therefore they are usually missing from the CHM tree density estimates.

Moreover, when performing a canopy segmentation using a marker controlled watershed algorithm over areas with missing trees, the canopy diameter estimates from the UAV-SfM tend to be slightly larger (although not significantly different for WP and natural areas of RRE) than those from the on-ground measurements at the lower end of the distribution (see Table 2 and Fig. 7d). This is because the detected treetops around which the canopies can propagate, tend to absorb the canopies of trees with highly overlapping crowns that have not been detected by the tree detection algorithm (Yin and Wang, 2019). This problem is accentuated on rehabilitated areas of RRE, which have a higher tree density than natural areas, and therefore have numerous non-detected trees whose canopies are absorbed by the adjacent trees. Consequently, canopy diameter obtained from the UAV-SfM data on rehabilitated areas of RRE was significantly larger than that obtained from on-ground data. This problem could be solved by applying a higher minimum threshold below which a canopy cannot propagate for the lower canopy story (0.9 instead of 0.8), which seems to cause the shifted distribution.

In spite of UAV imagery being collected one year after the on-ground measurements, tree height estimates from the UAV-SfM derived CHMs have an extremely close correspondence with field-derived measurements (Table 2). Mangrove tree heights and canopy diameters were not likely to change by > 5 to 10 cm due to the slow growth rate typical of mangroves in temperate and subtropical climates from one year to the next (Macnae, 1966). Additionally, DTM generation

averaged an RMSE of 6.3 and 9 cm lower when compared to the GCP heights (for WP and rehabilitated areas of RRE), which could explain the null difference of tree height medians from both methodologies. The higher RMSE for the DTM generation of natural areas of RRE is explained by the fact that less ground points are visible from the UAV point of view due to the higher canopy heights and coverage typical of mature natural areas. Ground points in these areas are usually found at the shoreline or behind the mangroves, and consequently DTM is usually generated by interpolation of these two areas. As mangrove ecosystems tend to accumulate mud in the ground, higher ground points than surrounding areas are expected to be found, which could lead to the DTM being underestimated by the UAV method. However, this method still performs better than other methodologies used on mangrove ecosystems (Otero et al., 2018, which used a fixed value for DTM generation of UAV data; or Fatoyinbo and Simard, 2013, which estimated Canopy height with an overall root mean square error of 3.55 m using free satellite data).

UAV-SfM derived AGB estimates also showed a strong relationship with on-ground measurements when using both all data and only top canopy data. However, the best fitted linear relationship for only top canopy (Fig. 8b) was closer to the ideal one-to-one relationship. UAV-SfM data tends to slightly underestimate AGB at low on-ground AGB estimates (< 100 t/ha), and slightly overestimate at high on-ground AGB estimates (> 100 t/ha). This is counterintuitive when combined with the results from the tree density estimates. Higher AGB estimates would be expected in areas with high tree densities (which had lower correlation with on-ground measured densities). However, closer inspection at the plot level revealed that the plots with higher tree densities are those in the initial stages of colonization, with immature or non-fully grown trees. These trees are on the low spectrum of height (< 1.5 m for WP and < 2 m for RRE) and canopy diameter (< 1 m for both areas) metrics and consequently, tend to be the ones with lower AGB estimates. As an example, one single tree of 4 m in height and 1.5 m in average canopy diameter holds more AGB than ten trees half its size on both measurements.

The AGB estimates created using the UAV-SfM methods described in this study were on average between 10 and 20% lower than those generated from the on-ground data at the site level in natural areas. This value is comparable to previous studies that use expensive LiDAR or laser scanning systems (Jaakkola et al., 2010; Sankey et al., 2017) or when assessing crops or plantation forests with clearly defined

boundaries between trees (Bendig et al., 2014; Li et al., 2016; Vega et al., 2015; Zahawi et al., 2015). Moreover, UAV-SfM data derived metrics (height, canopy diameter and AGB) obtained in this study had the highest correlation with on-ground measurements than any other previous studies with mangroves (Navarro et al., 2019; Otero et al., 2018).

4.2. Benefits of using UAV-SfM for retrieving forest inventory data from mangrove ecosystems

The main advantage of using UAVs for mangrove forest monitoring over traditional field measurements is the ability to survey broader spatial areas over a shorter period of time. A single UAV flight can cover an area of approximately 1 ha of forest in less than an hour (including flight planning and set up) and, if necessary, one person alone would be able to acquire all UAV data. In contrast, a team of five people with experience in field sampling would have to work 8 h per day over 31 days to survey the same area on the ground (estimates based on the time it took a team of 5 people to survey the 41 plots present in this study).

Similarly to savings in personnel, the cost saving benefits of using UAV-SfM technology for mangrove monitoring are significant when compared to on-ground measurements. The total cost for 100 days (average lifespan of UAV related technology) of surveys is AU\$ 57,040 cheaper for UAVs than for on-ground measurements (Table 3). This difference is accentuated when considering area covered, as UAV-SfM costs drop to just AU\$ 125 per ha, while on-ground costs are almost AU\$ 50 K per ha. Furthermore, despite having to do an initial investment of AU\$ 10,284 for equipment alone (which includes back up UAVs), UAV-SfM become cost-effective after just 15 days of surveys when compared to on-ground surveys (Fig. 9; AU\$ 23,816 vs AU\$ 24,154 respectively).

The UAV-SfM also facilitates monitoring of areas that are difficult to access, especially near the water's edge where mangrove trees tend to be higher and more densely packed. Moreover, UAVs are developing extremely fast and you can now buy a drone with RTK GPS incorporated for under AU\$ 10 K. While this might seem expensive, the imagery obtained from this drone will be georeferenced with very high precision without the need for placing GCPs on the ground, resulting in additional time and cost savings. While this technology is still developing, this price is likely to reduce in the near future, making it an even more cost-effective tool for monitoring mangrove ecosystems.

4.3. Limitations

This study has three major limitations, the first being that operation of UAVs is restricted to optimal conditions. To effectively operate an UAV, you need low wind speed (< 15 knots or 7.7 m/s), no rain, and low tides to ensure weather conditions will not interfere with data collection and processing. These restrictions greatly limit the amount of days conducive to surveying, which affects the frequency and costs associated with UAV surveys. Moreover, areas within no-fly zones (i.e. near airports) are restricted for surveying without a Remote Operator's Certificate (ReOC) license in Australia. Nonetheless, new changes to UAV laws in Australia have softened the requirements for remote-piloted aircraft under 2 kg (Allan et al., 2015).

The second limitation is that the UAV-method cannot detect understory trees and tends to saturate at high mangrove tree density. However, this limitation has a minor effect on the AGB estimations, as the non-detected trees tend to be the younger, not totally formed ones (whose heights and canopy diameters, and consequently AGB estimates, are on the lower end of the distribution) and hold on average only 9.1% of the total AGB.

The third limitation is that this method is still dependant on on-ground surveys to create the functions used to determine the variable window size on Step 1 and have a general idea of the survey area.

Nevertheless, our method can make use of previously obtained forest inventory data and also be implemented in areas with similar composition to those ground-based surveys. Additionally, an approach combining our UAV-SfM method with multispectral information and/or machine learning could be used to improve mangrove species identification and consequently the accuracy of the AGB estimates using species-specific allometric equations. This approach could potentially be implemented in other regions such as tropical areas where mangrove species composition is more diverse. However, this approach was outside the scope of this paper and could be the focus of future research.

5. Conclusions

Through this study, we showed that low-cost UAV-SfM provide an accurate and efficient method for assessing the above-ground biomass of mangrove forests in temperate and sub-tropical regions. We were able to obtain accurate tree height and canopy diameter metrics from UAV-SfM data that had a high correspondence with on-ground based data. The methods described in this study opens the possibility for easily repeatable, low-cost UAV surveys for local managers by providing a faster, more cost-effective approach for monitoring mangrove forests over larger areas than traditional on-ground surveys while maintaining forest inventory data accuracy. Additionally, as mangrove ecosystems in Australia are likely to be impacted by climate change related issues, the use of periodical UAV surveys for monitoring mangroves can lead to better restoration and management understanding under changing climatic conditions in temperate and sub-tropical areas.

CRedit authorship contribution statement

Alejandro Navarro: Conceptualization, Methodology, Software, Formal analysis, Investigation, Writing - original draft. **Mary Young:** Conceptualization, Writing - review & editing, Supervision. **Blake Allan:** Methodology, Writing - review & editing. **Paul Carnell:** Investigation, Data curation, Writing - review & editing. **Peter Macreadie:** Writing - review & editing, Supervision, Funding acquisition. **Daniel Ierodiaconou:** Conceptualization, Writing - review & editing, Supervision, Project administration, Funding acquisition.

Declaration of competing interest

The authors declare that they have no known competing financial interests or personal relationships that could have appeared to influence the work reported in this paper.

Acknowledgements

This study is part of the Mapping Ocean Wealth project from The Nature Conservancy's Great Southern Seascapes program and supported by The Thomas Foundation, HSBC Australia, the Ian Potter Foundation, and Victorian and New South Wales governments including Parks Victoria, Department of Environment Land Water and Planning, Victorian Fisheries Authority, New South Wales Office of Environment and Heritage, and New South Wales Department of Primary Industries. Funding was also provided by an Australian Research Council Linkage Project (LP160100242) and resources from the Victorian Coastal Monitoring Program.

References

- Allan, B.M., Ierodiaconou, D., Nimmo, D.G., Herbert, M., Ritchie, E.G., 2015. Free as a drone: ecologists can add UAVs to their toolbox. *Front. Ecol. Environ.* 13, 354–355.
- Alongi, D.M., 2008. Mangrove forests: resilience, protection from tsunamis, and responses to global climate change. *Estuarine Coastal and Shelf Science* 76, 1–13.
- Atwood, T.B., Connolly, R.M., Almahasheer, H., Carnell, P.E., Duarte, C.M., Lewis, C.J.E., Irigoien, X., Kelleway, J.J., Lavery, P.S., Macreadie, P.I., 2017. Global patterns in

- mangrove soil carbon stocks and losses. *Nat. Clim. Chang.* 7, 523.
- Badola, R., Hussain, S.A., 2005. Valuing ecosystem functions: an empirical study on the storm protection function of Bhitarkanika mangrove ecosystem, India. *Environ. Conserv.* 32, 85–92.
- Barthelme, S., 2018. *Imager: Image Processing Library Based on 'Clmg'*. R Package Version 0.41.1, 2 pp. 357.
- Bendig, J., Bolten, A., Bennertz, S., Broscheit, J., Eichfuss, S., Bareth, G., 2014. Estimating biomass of barley using crop surface models (CSMs) derived from UAV-based RGB imaging. *Remote Sens.* 6, 10395–10412.
- Bergstrom, J.C., Stoll, J.R., Titre, J.P., Wright, V.L., 1990. Economic value of wetlands-based recreation. *Ecol. Econ.* 2, 129–147.
- Boon, P., Allen, T., Brook, J., Carr, G., Frood, D., Harty, C., Hoye, J., McMahon, A., Mathews, S., Rosengren, N., 2011. *Victorian Saltmarsh Study: Mangroves and Coastal Saltmarsh of Victoria: Distribution, Condition, Threats and Management*. Institute for Sustainability and Innovation, Victoria University, Melbourne, Australia.
- Clark, G.F., & Johnston, E.L., 2016. *Coasts*. In *Australia state of the environment* (Ed.). Australian Government Department of the Environment and Energy, Canberra: <https://soe.environment.gov.au/theme/coasts>.
- Dandois, J.P., Ellis, E.C., 2010. Remote sensing of vegetation structure using computer vision. *Remote Sens.* 2, 1157–1176.
- Dandois, J.P., Ellis, E.C., 2013. High spatial resolution three-dimensional mapping of vegetation spectral dynamics using computer vision. *Remote Sens. Environ.* 136, 259–276.
- Das, S., Vincent, J.R., 2009. Mangroves protected villages and reduced death toll during Indian super cyclone. *Proc. Natl. Acad. Sci. U. S. A.* 106, 7357–7360.
- Donato, D.C., Kauffman, J.B., Murdiyaro, D., Kurnianto, S., Stidham, M., Kanninen, M., 2011. Mangroves among the most carbon-rich forests in the tropics. *Nat. Geosci.* 4, 293–297.
- Duncan, C., Primavera, J.H., Pettorelli, N., Thompson, J.R., Loma, R.J.A., Koldewey, H.J., 2016. Rehabilitating mangrove ecosystem services: a case study on the relative benefits of abandoned pond reversion from Panay Island, Philippines. *Mar. Pollut. Bull.* 109, 772–782.
- Dustin, M.C., 2015. *Monitoring Parks with Inexpensive UAVs: Cost Benefits Analysis for Monitoring and Maintaining Parks Facilities*. University of Southern California.
- Fatoyinbo, T.E., Simard, M., 2013. Height and biomass of mangroves in Africa from ICESat/GLAS and SRTM. *Int. J. Remote Sens.* 34, 668–681.
- Feliciano, E.A., Wdowinski, S., Potts, M.D., 2014. Assessing mangrove above-ground biomass and structure using terrestrial laser scanning: a case study in the Everglades National Park. *Wetlands* 34, 955–968.
- Fu, W., Wu, Y., 2011. Estimation of aboveground biomass of different mangrove trees based on canopy diameter and tree height. *Procedia Environ. Sci.* 10, 2189–2194.
- Giri, C., 2016. Observation and monitoring of mangrove forests using remote sensing: opportunities and challenges. *Remote Sens.* 8, 8.
- Hamilton, S.E., Casey, D., 2016. Creation of a high spatio-temporal resolution global database of continuous mangrove forest cover for the 21st century (CGMFC-21). *Glob. Ecol. Biogeogr.* 25, 729–738.
- Hemminga, M.A., Duarte, C.M., 2000. *Seagrass Ecology*. Cambridge University Press.
- Hollister, J.W., 2018. *Lakemorpho: Lake Morphometry Metrics*. R package version 1.1.1. <https://CRAN.R-project.org/package=lakemorpho>.
- Jaakkola, A., Hyyppä, J., Kukko, A., Yu, X.W., Kaartinen, H., Lehtomäki, M., Lin, Y., 2010. A low-cost multi-sensoral mobile mapping system and its feasibility for tree measurements. *ISPRS J. Photogramm. Remote Sens.* 65, 514–522.
- Koch, E.W., Barbier, E.B., Silliman, B.R., Reed, D.J., Perillo, G.M.E., Hacker, S.D., Granek, E.F., Primavera, J.H., Muthiga, N., Polasky, S., Halpern, B.S., Kennedy, C.J., Kappel, C.V., Wolanski, E., 2009. Non-linearity in ecosystem services: temporal and spatial variability in coastal protection. *Front. Ecol. Environ.* 7, 29–37.
- Kuenzer, C., Bluemel, A., Gebhardt, S., Quoc, T.V., Dech, S., 2011. Remote sensing of mangrove ecosystems: a review. *Remote Sens.* 3, 878–928.
- Lee, K., Lunetta, R.S., 1995. Wetland detection methods. In: Lyon, J.G., McCarthy, J. (Eds.), *Wetland and Environmental Applications in GIS*. Lewis, Boca Raton, Florida, pp. 249–284.
- Li, W., Niu, Z., Chen, H.Y., Li, D., Wu, M.Q., Zhao, W., 2016. Remote estimation of canopy height and aboveground biomass of maize using high-resolution stereo images from a low-cost unmanned aerial vehicle system. *Ecol. Indic.* 67, 637–648.
- Macnae, W., 1966. Mangroves in eastern and southern Australia. *Aust. J. Bot.* 14 (67–&).
- Manfreda, S., McCabe, M.F., Miller, P.E., Lucas, R., Pajuelo Madrigal, V., Mallinis, G., Ben Dor, E., Helman, D., Estes, L., Ciraolo, G., 2018. On the use of unmanned aerial systems for environmental monitoring. *Remote Sens.* 10, 641.
- Matese, A., Toscano, P., Di Gennaro, S., Genesio, L., Vaccari, F., Primicerio, J., Belli, C., Zaldei, A., Bianconi, R., Gioli, B., 2015. Intercomparison of UAV, aircraft and satellite remote sensing platforms for precision viticulture. *Remote Sens.* 7, 2971–2990.
- McLeod, G., Chmura, G.L., Bouillon, S., Salm, R., Björk, M., Duarte, C.M., Lovelock, C.E., Schlesinger, W.H., Silliman, B.R., 2011. A blueprint for blue carbon: toward an improved understanding of the role of vegetated coastal habitats in sequestering CO₂. *Front. Ecol. Environ.* 9, 552–560.
- Messinger, M., Asner, G.P., Silman, M., 2016. Rapid assessments of Amazon forest structure and biomass using small unmanned aerial systems. *Remote Sens.* 8, 615.
- Murfit, S.L., Allan, B.M., Bellgrove, A., Rattray, A., Young, M.A., Ierodiakonou, D., 2017. Applications of unmanned aerial vehicles in intertidal reef monitoring. *Sci. Rep.* 7, 11.
- Nam, V.N., Sasmito, S.D., Murdiyaro, D., Purbopuspito, J., MacKenzie, R.A., 2016. Carbon stocks in artificially and naturally regenerated mangrove ecosystems in the Mekong Delta. *Wetl. Ecol. Manag.* 24, 231–244.
- Navarro, J.A., Algeet, N., Fernandez-Landa, A., Esteban, J., Rodriguez-Noriega, P., Guillen-Climent, M.L., 2019. Integration of UAV, Sentinel-1, and Sentinel-2 data for mangrove plantation aboveground biomass monitoring in Senegal. *Remote Sens.* 11, 23.
- Nesbit, P.R., Hugenholz, C.H., 2019. Enhancing UAV-SfM 3D model accuracy in high-relief landscapes by incorporating oblique images. *Remote Sens.* 11, 239.
- Nevalainen, O., Honkavaara, E., Tuominen, S., Viljanen, N., Hakala, T., Yu, X.W., Hyyppä, J., Saari, H., Polonen, I., Imai, N.N., Tommaselli, A.M.G., 2017. Individual tree detection and classification with UAV-based photogrammetric point clouds and hyperspectral imaging. *Remote Sens.* 9, 34.
- Otero, V., Van De Kerchove, R., Satyanarayana, B., Martinez-Espinoso, C., Bin Fisol, M.A., Bin Ibrahim, M.R., Sulong, I., Mohd-Lokman, H., Lucas, R., Dandouh-Guebas, F., 2018. Managing mangrove forests from the sky: forest inventory using field data and Unmanned Aerial Vehicle (UAV) imagery in the Matang Mangrove Forest Reserve, peninsular Malaysia. *For. Ecol. Manag.* 411, 35–45.
- Owers, C.J., Rogers, K., Woodroffe, C.D., 2018. Spatial variation of above-ground carbon storage in temperate coastal wetlands. *Estuar. Coast. Shelf Sci.* 210, 55–67.
- Panagiotidis, D., Abdollahnejad, A., Surovy, P., Chiteculo, V., 2017. Determining tree height and crown diameter from high-resolution UAV imagery. *Int. J. Remote Sens.* 38, 2392–2410.
- Pham, T.D., Yokoya, N., Bui, D.T., Yoshino, D.A., 2019. Remote sensing approaches for monitoring mangrove species, structure, and biomass: opportunities and challenges. *Remote Sens.* 11, 24.
- Pix4D SA. *Pix4Dmapper*. Available online: <https://www.pix4d.com/product/pix4dmapperphotogrammetry-software> (accessed on 18 November 2019).
- Popescu, S.C., Wynne, R.H., 2004. Seeing the trees in the forest: using lidar and multi-spectral data fusion with local filtering and variable window size for estimating tree height. *Photogramm. Eng. Remote Sens.* 70, 589–604.
- Ren, H., Chen, H., Li, Z., Han, W., 2010. Biomass accumulation and carbon storage of four different aged Sonneratia apetala plantations in Southern China. *Plant Soil* 327, 279–291.
- Richards, D.R., Friess, D.A., 2016. Rates and drivers of mangrove deforestation in Southeast Asia, 2000–2012. *Proc. Natl. Acad. Sci.* 113, 344–349.
- Roussel, J., Auty, D., 2018. *lidR: Airborne LiDAR Data Manipulation and Visualization for Forestry Applications*. R Package Version 2.0.0.
- Russell, K., 2005. *NSW Northern Rivers Estuary Habitat Mapping-Final Analysis Report*. NSW Department of Primary Industries, Port Stephens.
- Ruwaimana, M., Satyanarayana, B., Otero, V., Muslim, A.M., Syafiq, A.M., Ibrahim, S., Raymaekers, D., Koedam, N., Dahdouh-Guebas, F., 2018. The advantages of using drones over space-borne imagery in the mapping of mangrove forests. *PLoS ONE* 13, 22.
- Samiappan, S., Turnage, G., Hathcock, L., Casagrande, L., Stinson, P., Moorhead, R., 2016. Using unmanned aerial vehicles for high-resolution remote sensing to map invasive *Phragmites australis* in coastal wetlands. *Int. J. Remote Sens.* 1–19.
- Sankey, T., Donager, J., McVay, J., Sankey, J.B., 2017. UAV lidar and hyperspectral fusion for forest monitoring in the southwestern USA. *Remote Sens. Environ.* 195, 30–43.
- Shapiro, S.S., Wilk, M.B., 1965. An analysis of variance test for normality (complete samples). *Biometrika* 52, 591.
- Sperlich, M., Kattenborn, T., Koch, B., Kattenborn, G., 2014. Potential of unmanned aerial vehicle based photogrammetric point clouds for automatic single tree detection. *Gemeinsame Tagung* 1–6.
- Thomas, N., Lucas, R., Bunting, P., Hardy, A., Rosenqvist, A., Simard, M., 2017. Distribution and drivers of global mangrove forest change, 1996–2010. *PLoS One* 12, 14.
- Tian, J.Y., Wang, L., Li, X.J., Gong, H.L., Shi, C., Zhong, R.F., Liu, X.M., 2017. Comparison of UAV and WorldView-2 imagery for mapping leaf area index of mangrove forest. *Int. J. Appl. Earth Obs. Geoinf.* 61, 22–31.
- Vandervalk, A.G., Attiwill, P.M., 1984. Decomposition of leaf and root litter of *Avicennia marina* at Westport Bay, Victoria, Australia. *Aquat. Bot.* 18, 205–221.
- Vega, F.A., Ramirez, F.C., Saiz, M.P., Rosua, F.O., 2015. Multi-temporal imaging using an unmanned aerial vehicle for monitoring a sunflower crop. *Biosyst. Eng.* 132, 19–27.
- Vincent, L., Soille, P., 1991. Watersheds in digital spaces - an efficient algorithm based on immersion simulations. *IEEE Trans. Pattern Anal. Mach. Intell.* 13, 583–598.
- Wallace, L., Lucier, A., Malenovsky, Z., Turner, D., Vopenka, P., 2016. Assessment of Forest structure using two UAV techniques: a comparison of airborne laser scanning and structure from motion (SfM) point clouds. *Forests* 7, 16.
- Wang, L., Jia, M.M., Yin, D.M., Tian, J.Y., 2019. A review of remote sensing for mangrove forests: 1956–2018. *Remote Sens. Environ.* 231, 15.
- Wannasiri, W., Nagai, M., Honda, K., Santitammont, P., Miphokasap, P., 2013. Extraction of mangrove biophysical parameters using airborne LiDAR. *Remote Sens.* 5, 1787–1808.
- Ward, R., Burnside, N., Joyce, C., Sepp, K., Teasdale, P., 2016. Improved modelling of the impacts of sea level rise on coastal wetland plant communities. *Hydrobiologia* 774, 203–216.
- Westoby, M.J., Brasington, J., Glasser, N.F., Hambrey, M.J., Reynolds, J.M., 2012. 'Structure-from-motion' photogrammetry: a low-cost, effective tool for geoscience applications. *Geomorphology* 179, 300–314.
- Wilcoxon, F., 1992. Individual comparisons by ranking methods. In: *Breakthroughs in Statistics*. Springer, pp. 196–202.
- Yaney-Keller, A., Tomillo, P.S., Marshall, J.M., Paladino, F.V., 2019. Using Unmanned Aerial Systems (UAS) to assay mangrove estuaries on the Pacific coast of Costa Rica. *PLoS One* 14, e0217310.
- Yin, D., Wang, L., 2019. Individual mangrove tree measurement using UAV-based LiDAR data: possibilities and challenges. *Remote Sens. Environ.* 223, 34–49.
- Zahawi, R.A., Dandois, J.P., Holl, K.D., Nadwodny, D., Reid, J.L., Ellis, E.C., 2015. Using lightweight unmanned aerial vehicles to monitor tropical forest recovery. *Biol. Conserv.* 186, 287–295.
- Zarco-Tejada, P.J., Diaz-Varela, R., Angileri, V., Loudjani, P., 2014. Tree height quantification using very high resolution imagery acquired from an unmanned aerial vehicle (UAV) and automatic 3D photo-reconstruction methods. *Eur. J. Agron.* 55, 89–99.
- Zhang, K.Q., Chen, S.C., Whitman, D., Shyu, M.L., Yan, J.H., Zhang, C.C., 2003. A progressive morphological filter for removing nonground measurements from airborne LiDAR data. *IEEE Trans. Geosci. Remote Sens.* 41, 872–882.